E13-2002-138

R. A. Astabatyan[1], R. Kalpakchieva, R. L. Kavalov[1],
A. Kugler[2], I. V. Kuznetsov, V. F. Kushniruk,
S. P. Lobastov, S. M. Lukyanov, E. R. Markaryan[1],
V. A. Maslov, L. Mikhailov[2], Yu. E. Penionzhkevich,
N. O. Poroshin[3], N. K. Skobelev, V. I. Smirnov,
Yu. G. Sobolev, V. Yu. Ugryumov

SET-UP ON THE BASIS OF MULTIWIRE PROPORTIONAL AND IONIZATION CHAMBERS FOR RADIOACTIVE BEAM EXPERIMENTS

Submitted to «Nuclear Instruments and Methods A»

[1]Yerevan Physical Institute, Yerevan, Armenia
[2]Nuclear Physics Institute, Rež, Czech Republic
[3]Moscow Engineering Physics Institute, Russia

Introduction

The MULTI set-up [1, 2] is intended for experiments on studying the properties of exotic nuclei like elastic (inelastic) scattering, the break-up of the nucleus into its constituent clusters. Experiments of that kind generally require not only spectroscopic measurement but also measurement of the angular distributions of reaction products; it is also necessary to identify correlated particles and find the angle between them. The most reliable technique to carry out those measurements is to reconstruct trajectories by repeatedly determining particle positions along tracks. Using multiwire proportional chambers (MWPCs) for that purpose has the following advantages:

— the small amount of MWPCs matter provided the minimal energy and angular straggling of detected particles;

— decreased background due to the accompanying reactions upstream of the target and on the detectors by means of trajectory reconstruction and selecting them on the scattering centre (target);

— wide-aperture measurement of reaction products against primary beam background;

— trigger generation on interaction of particles to enable relatively large scattering angle measurement;

— reconstruction of the trajectories of incident particles (or "active" collimation, which restricts the beam dimensions) onto the target.

To fulfil the above tasks and purposes, a system of coordinate MWPCs has been created. It allows beam profile measurement, making it possible the position of each incident particle to be determined (event by event), reaction particle trajectory reconstruction and angular distribution determination.

In addition, the system is equipped with a longitudinal drift ionization chamber, as an alternative to solid-state detectors of large areas, for dE/dx measurement.

Tests

There are a lot of works devoted to MWPCs. The fundamentals of MWPCs were considered in work [3]. The design of the MWPCs under discussion, which are intended to be used with the MULTY set-up, meets the severe constraint on the amount of matter contained in them imposed by operation in conjunction with experimental nuclear physics set-ups. Therefore:

–light gas of as low as possible pressure, which is variable, is employed;

–cathodes are thin conducting films;

–MWPCs are one unit, to decrease the number of windows, which are scattering centres, and positioned in the reaction chamber.

From the design standpoint, all type of MWPCs are identical and differ only in size. Fig. 1 presents a general view of one of the MWPC. The distance between anode-cathode is 6 mm. The cathodes are solid 3 μm metallized mylar electrodes. The signal wires, 20 μm in diameter, are stretched with 2 mm spacing.

Beam tests of a MWPC were conducted on the U-400M heavy-ion accelerator [2]. Reaction products (^{12}C(42 MeV/A) + Au) were detected at an angle of 8° relative to the beam axis.

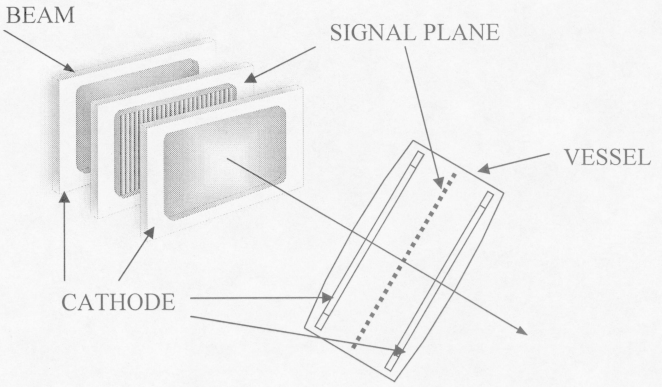

Fig. 1. *General view of one of the MWPC coordinates.*

Fig. 2 presents the MWPC counting characteristic for $1 \leq Z \leq 6$ fragments, which were detected. The intensity of the heaviest particle (^{12}C) was ~ 10^3 1/s per wire. The counting characteristic presented was measured in the energy range E=(10-500) MeV for the all fragments. It should be noted that the limiting value of voltage, U=3.8 kV, corresponds to a detection efficiency of ~90% for electrons from the ^{90}Sr isotope.

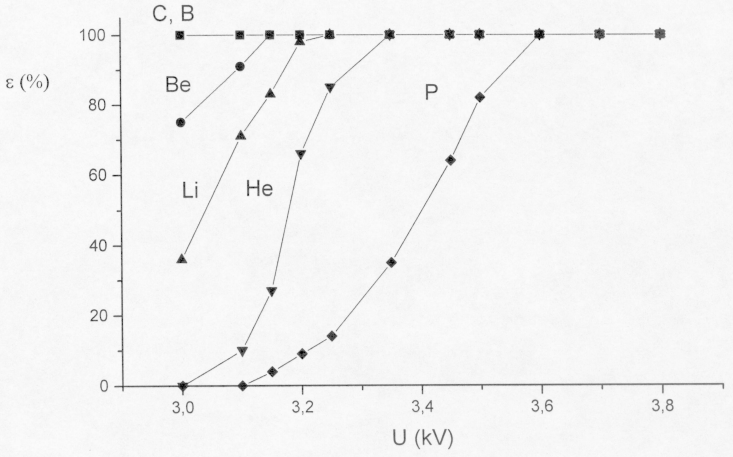

Fig. 2. *MWPC counting characteristic for various type of detected fragment*

When ions with the wide range of Z are detected, this causes the formation of an enormous spatial charge around the wire. Its long dispersal time sharply reduces the MWPC counting ability by approximately a factor of the ratio of the ionizing powers of lightest and heaviest ions. As a result, in our case (see Fig.2) the counting ability falls from the nominal (~$5x10^5$ 1/s per wire for particles with the same charge) to (10^3 – 10^4) s^{-1}. We note that, the operating mode of MWPC corresponds to the U=3.6 kV of the counting characteristic in Fig. 2 and the proton detection efficiency was near 100%.

The time resolution for the set of particles presented in Fig. 2 is equal or better than 20 ns. The position (angular) resolution is determined by the cell X, Y dimensions, which are (2x2) mm^2, as well as by the average number of channel multiple operations. In this case coordinate reconstruction was done based on the centre of gravity of the wires that had operated. Obviously, multiple operation probability depends on the type of detected particle, its values for light and heavy particles differing significantly.

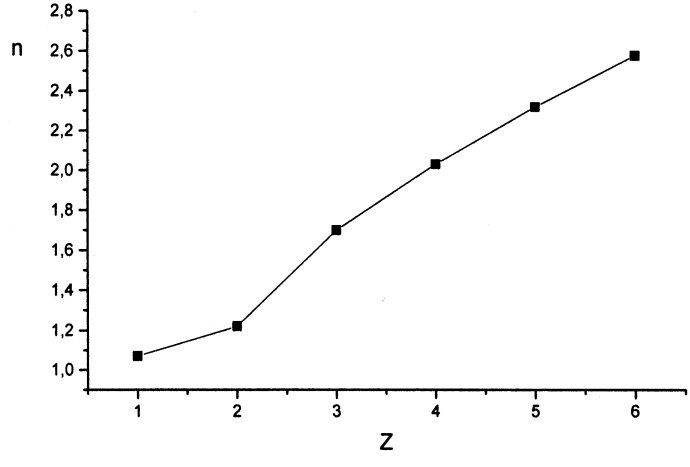

Fig. 3. *Average number of channel operations as a function of particle charge Z*

Fig. 3 shows the Z-dependence of the average number of channel operations for the particles of Fig. 2. Those data permit making an estimate of the two-track position resolution for correlated pairs of a chosen Z.

The MWPC operates with stationary gas filling. The gas filling was a mixture of Ar and CH_4 or pure CH_4. The chamber filling cycle depends heavily on the degree to which the chamber is vacuum-pumped before being filled and how tight it is. For the vacuum-pumping and tightness that were achieved the signal amplitude fell by (20-30)% in the first twenty-four hours after filling and then decreased near-exponentially. This allows stable operation for more than 15 days in the U=3.7 kV mode and a proton detection efficiency of ~100%. The gas mixture pressure is variable in the range from 0.1 to 1 atm depending on particle ionizing capacity.

In particular, the stable mode of near 100% ^{6}He detection efficiency is provided with pure CH_4 at P=0.1 atm.

Experimental set-up

Fig.4 gives a general view of the secondary-beam separation and formation channel[4]. A secondary beam of ^{6}He, T is produced in the interaction of a 34 MeV/A ^{7}Li initial beam with a 1.5 mm ^{9}Be production target. On being separated by Z and A through rigidity selection, the utilisation of a degrader of the suitable thickness and then being formed by an ion-optical system, the beam is directed to the target.

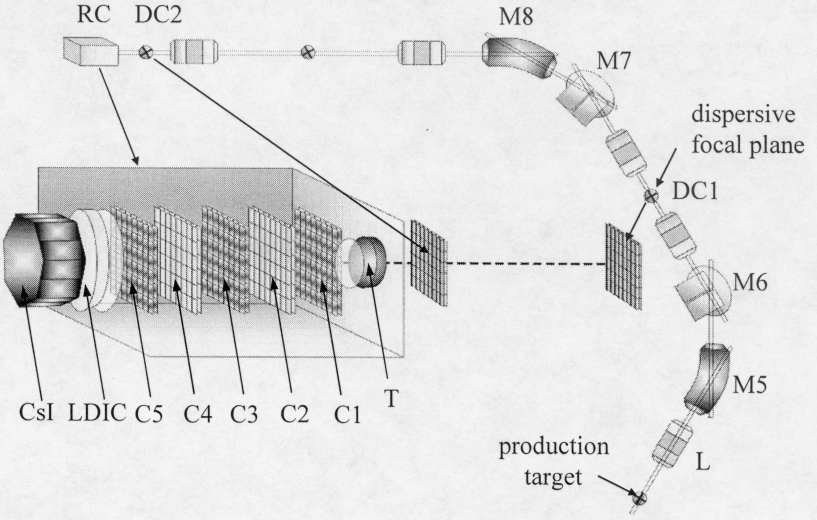

Fig. 4. *General view of the secondary beam separation and formation channel with the MULTI set-up*
DC1 and DC2-diagnostic MWPCs; RC- reaction chamber; LDIC- longitudinal drift ionization chamber; (C1-C5)- set of MWPCs; T- target.

To measure the beam profile in the focal plane and the immediate vicinity of the target (T), two two-coordinate MWPCs (DC1, DC2), which serve as diagnostic chambers, are installed. DC2 can also serve as an element of the data collection system or the event selection logic, providing narrow beam formation. The second and main part of the set-up is a reaction chamber (RC), which can house up to five two-coordinate MWPC modules (C1 – C5). They are intended for position separation of reaction products, trajectory reconstruction and scattering centre determination. To have an increased aperture angle for θ, the target can be positioned between modules (C2 – C5) inside the RC. Depending on the position of the target and the coordinate detectors, the RC aperture angles may be as much as $\theta_L \approx 30°$ and $\varphi \approx 2\pi$. The RC entrance window, 3 cm in diameter, also serves as a collimator to eliminate the beam halo. On the RC

(12x12) cm^2 exit window, there is a spectrometric unit mounted, which is consisted of longitudinal drift ionization chamber (LDIC) and CsI crystal, intended for identification and total energy measurement. In addition, a multisection ionization calorimeter is planned to be installed between MWPCs (C1-C5) for multiple measurement of ionization losses.

All the windows (the entrance and exit windows of DC1, DC2, RC and LDIC) are 7 μm mylar; if necessary, supporting meshes of 98% transparency can be used. It should be noted that measurement is carried out without the supporting meshes.

Let us take a look at the individual components of the set-up.

I. Beam-profile-measurement MWPCs (DC1, DC2)

Both DC1, DC2 consists of two (X, Y)-coordinate MWPC placed in a common vacuum-tight volume. This volume is placed in the diagnostic block on a pneumatic tube and can be installed into the set-up without vacuum failure. The useful area of the chamber is (60x60) mm^2 and form 30 (X) + 30 (Y) data channels.

The detection electronics consists of a preamplifier and a discriminator for each channel, the channel numbers being encoded and the data being transmitted to a PC. The readout logic is started with a fast trigger.

The main functions of the DCs are:

1. To measure and control the secondary beam profile. Fig. 5 presents on-line beam profiles from DC1 data.

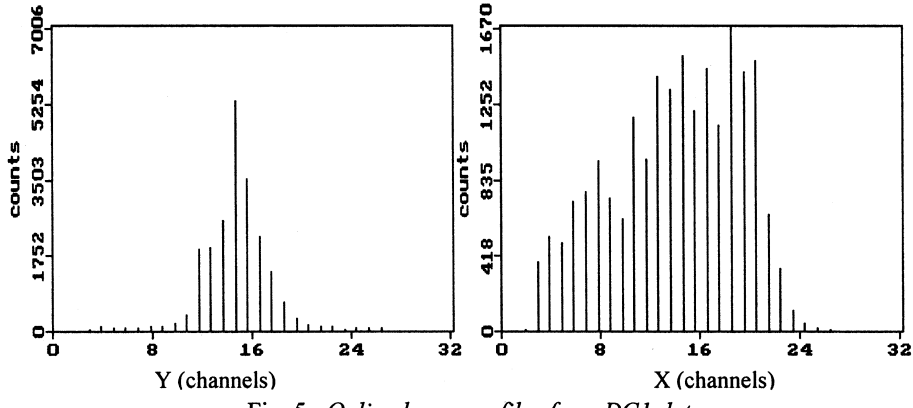

Fig. 5. *Online beam profiles from DC1 data*

2. To form a narrow beam onto the target by including an "active" collimator into the trigger generation logic. Fig. 6 shows "active" collimation with DC2 in action: 9 elementary cells are projected onto one of the chambers of the RC. Collimation of that kind excludes the beam background due to possible scattering centres on the way to the target. That a narrow input beam can be formed is especially important and necessary for detection at small scattering angles, which is characterised by the fact that the contribution from the angular divergence and general dimensions of the beam is likely to become dominant.

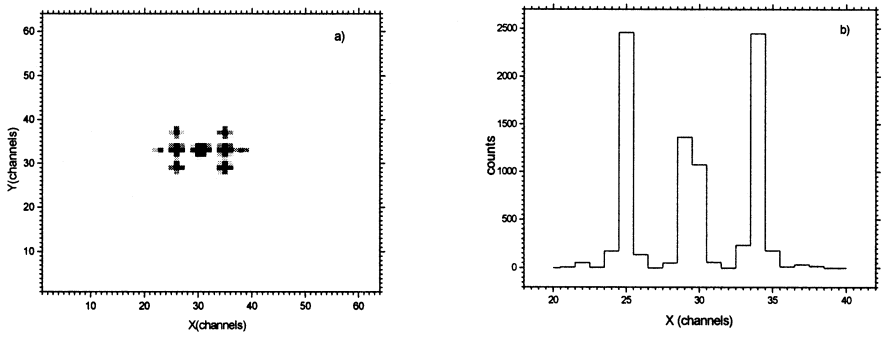

Fig. 6. *Two-dimensional (a) and linear (b) spectra from one of the chambers of the RC in the case of "active" collimation with DC2*

3. To generally monitor the beam in order to measure absolute cross sections of reactions.

4. To use DC for coordinate measurement at the dispersive focal plane in order to correct magnetic rigidity Bρ. How efficiently can be make such correction demonstrated the two-dimensional spectra of fragments (Fig.7) with correction (b) and without it (a). The results were obtained at LISE-2000 spectrometer by a reaction of fragmentation of 60A MeV ^{48} Ca beam in the frame of collaboration JINR-GANIL.

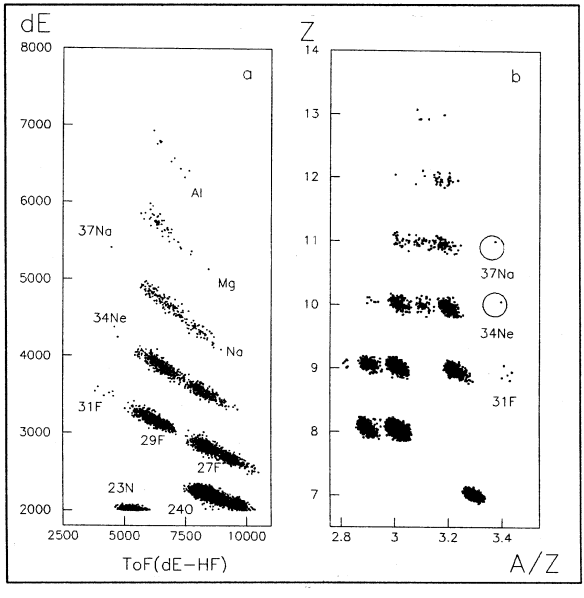

Fig.7. Two-dimensional spectra of fragments

II. **Reaction product detection MWPCs (C1 - C5)**

Each (C1-C5) has 60 (X) and 60 (Y) data channels and operating area (120x120) mm^2 and consists of two (X, Y)-coordinate MWPC placed in a common vacuum-tight volume RC (see Fig.4). The RC is 400 mm in length.

The readout system for the MWPCs is based on the RPC-32 analog electronic units developed at JINR [5]. In its functional capabilities, the RPC-32 is similar to the PCOS II systems and has 32-channel containing the input pulse-shaping preamplifiers and memory with a total capacity of (32 x 16)-bit words. There is a possibility of measuring the time coordinate of the recorded event. The coordinate-reading time is ~ 400 μs. The MWPC outputs are connected to the cards via ribbon cables 1 m long. The data readout logic is represented schematically in Fig. 8. It in particular allows one to use fast OR signals from every card and generate an MWPC data readout trigger signal (trigger2) for MWPCs as well as for the entire MULTI set-up if needed.

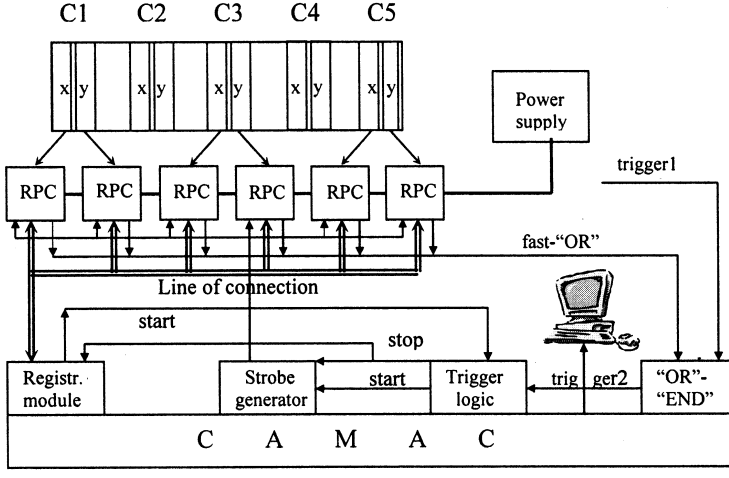

Fig. 8. *Data readout logic*

RPC- signal registration card; Registr. Module- readout controller with a buffer; "OR"-"END"- program-controlled logic unit

The (C1-C5) system in the MULTI set-up is intended mainly for coordinate measurements: position separation of particles, trajectory reconstruction, and determination of the angular spread between the correlated particles.

In addition to those main functions, on-line and off-line event selection is provided.

The off-line event selection criterion is for a track to be rectilinear by means of standard-program-based fitting being used [6]. This kind of selection allows one to suppress the contribution due to interactions in the detection system (interactions inside the RC) as well as exclude likely background and accidental events in every plane.

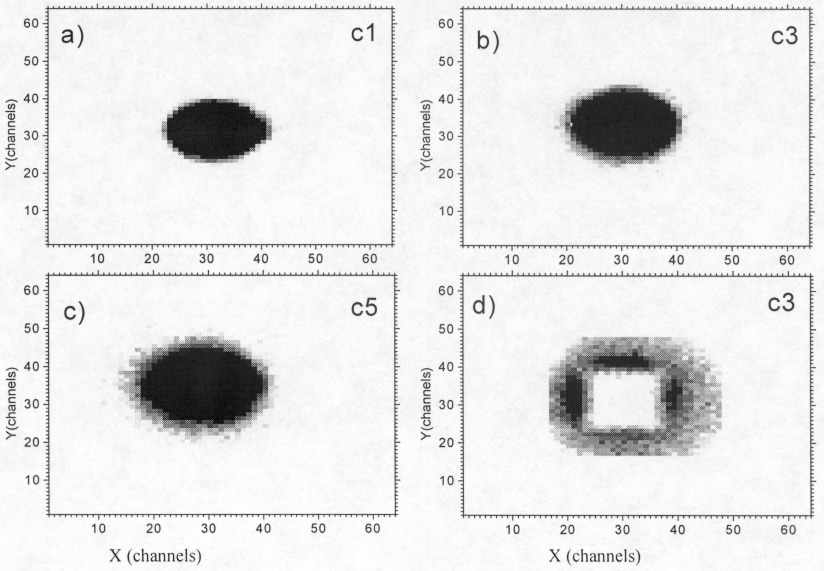

Fig. 9. *Two-dimensional spectra from the chambers on rectilinearity selection (a, b, c) and scattered particle selection (d)*

In Fig. 9a, b, c are presented two-dimensional spectra from the chambers. In Fig. 9d is illustrated the capability of using the second level trigger that permits selecting scattered particles. To perform this selection, the trigger for the set-up included a fast "OR" from the X, Y planes of C5, the central channels that correspond to the effective position of the incident beam being switched off.

An essential feature of the track system is that it can determine the position of the scattering centre (target) by projecting a detected particle onto the target. Fig. 10 presents the number of particles detected within a prescribed scattering angle as a function of the reconstructed scattering centre coordinate, Z. From here on, the centre of the coordinate system is at the geometrical centre of the target. It is obvious that the efficiency of such selection essentially depends both on the beam dimensions and on the scattering angle.

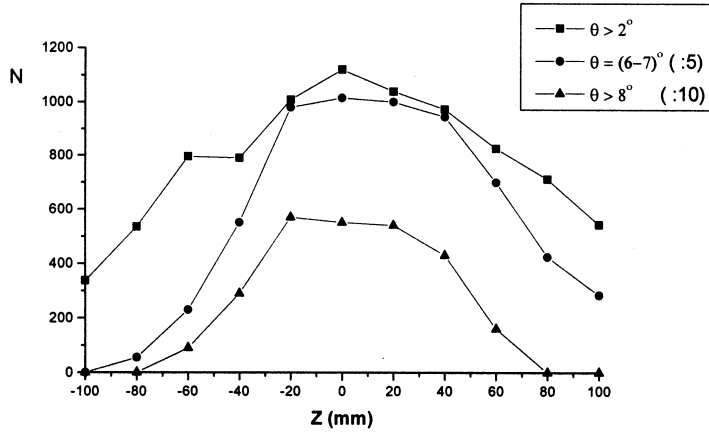

Fig. 10. *Number of detected particles as a function of the reconstructed scattering centre coordinates for different scattering angles*

III. **Wide-aperture longitudinal drift ionization chamber (LDIC)**

The chamber is an extended and modified version of a detector for detecting and identifying nuclear photofragmentation products [7]. It consists of a drift section with a longitudinal electrostatic field, Frish grid, and a detection anode.

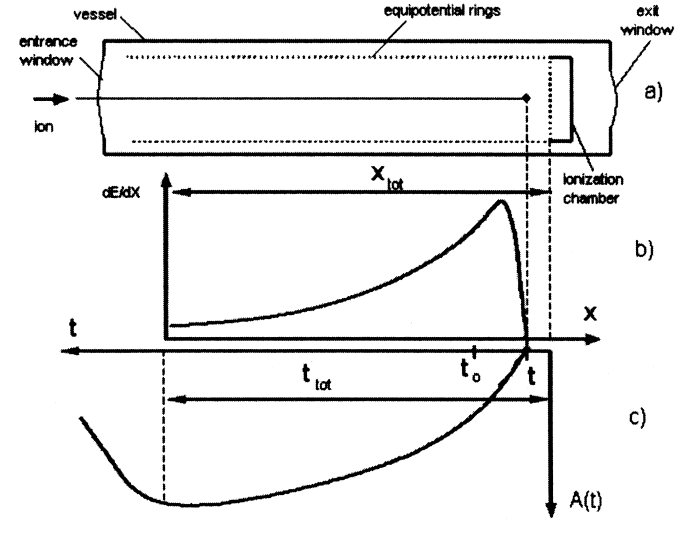

Fig. 11. *Design and operation of the LDIC*

The chamber design is represented schematically in Fig. 11a. The drift section is a cylinder with conducting strips, which serve as electrodes to create a uniform electrostatic field. The entrance and exit windows are 12 cm in diameter and made of 7 μm mylar. The anode is made of 3 μm aluminised mylar. The chamber length can be varied over a 300 mm range. ΔE identification of passing particles and complete ΔE, E, R (pathlength) identification of particles at rest can be carried out by measuring the pulse shape along the particle path.

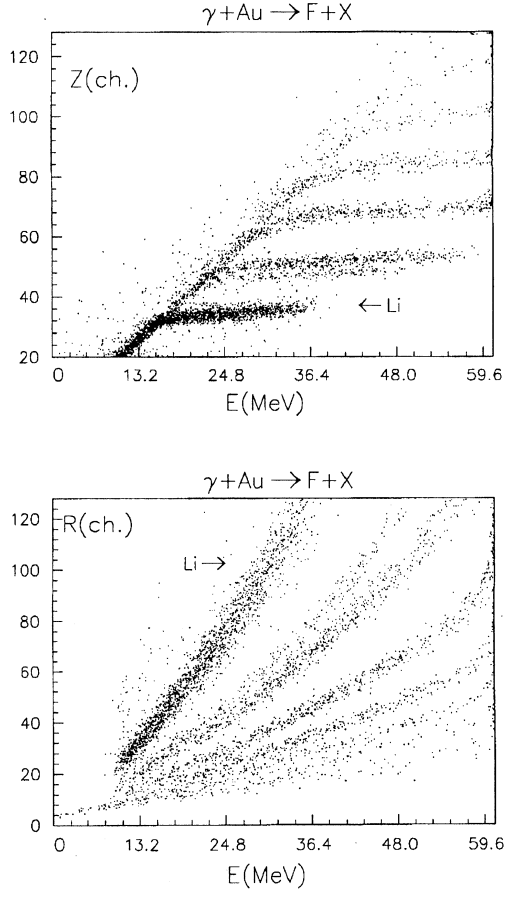

Fig. 12. *Two-dimensional (E, Z) and (E, R) spectra of products for photofragmentation on Au*

Fig. 11c shows a representative ionisation loss (dE/dx) curve for an absorbed ion, the corresponding collecting anode signal being given in Fig. 11c. From Fig. 11b, c, it is easy to obtain the following simple relationships: $E \sim A(t_{tot})$; $R=X_{tot}(1-t/t_{tot})$. It should be noted that ΔE measured relative to the path end is independent of particle energy.

This allows reliable particle identification by $Z \sim A(t_0)$ and, in part, isotope resolution as well. In Fig. 12 are presented the two-dimensional (E, Z) and (E, R) product spectra for the nuclear photofragmentation of Au from [8], as an example of the capability of identifying particles absorbed in the chamber.

The chamber of this type can be used:

1. As an alternative to multilayer semiconductor telescopes, which are commonly employed as detection targets in experiments on ^{6}He break-up at low energies close to the Coulomb barrier. In Fig. 13 is presented a test energy spectrum from a collimated (within the LDIC aperture) ^{226}Ra source. The α-source was positioned on the exterior side of the chamber entrance window. The energy resolution is ~ (150-200) KeV and basically governed by the preamplifier noises and the chamber entrance window energy loss fluctuations.

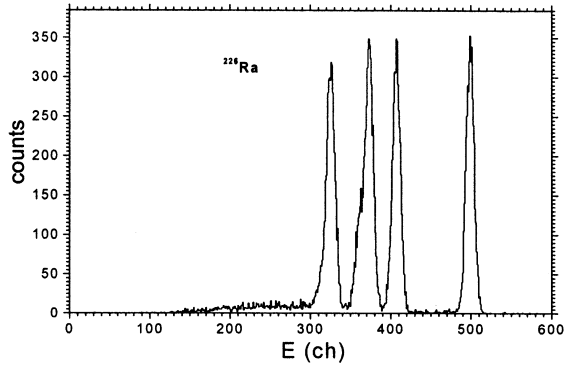

Fig. 13. *α-particle energy spectrum for a collimated ^{226}Ra source*

The chamber working gas can serve as a detection target. On the other hand, when operated in the ionization mode, the chamber can be filled with spectrally pure He, Ar, Kr, Xe allows a wider choice of target nuclei in comparision of multilayer semiconductor telescopes . Another essential advantage is that the detector absorption length can be varied by merely changing the gas pressure. 8 MeV/A ^{6}He is completely absorbed in a chamber of 30 cm length filled with pure Xe at a pressure of 2.5 atm, which is the maximum achieved in the chamber of the design under discussion.

2. For detection and identification of fission products in appropriate experiments. Fig. 14 shows the energy spectrum of noncollimated ^{252}Cf fission fragments for a source positioned inside the chamber. It should be noted that in such experiments the transparency for incident particles can be maximised by varying the gas pressure.

3. For ΔE identification of passing particles up until they are absorbed in the E detector. The above experimental set-up (Fig. 4) included an LDIC thus modified. The chamber was about 10 cm in length, the working gas being pure Ar at atmospheric pressure. The total collection (drift) time was about 2 μs. Fig. 15 presents a (ΔE, E) two-dimensional matrix of ionization losses ΔE for the LDIC and of total energy (E)

for CsI obtained in tests. The ^{6}He+T secondary beam maximal energy was about 70-80 MeV. In Fig. 15, ^{4}He, likely to have been produced in a ^{6}He break-up, is unambiguously identifiable.

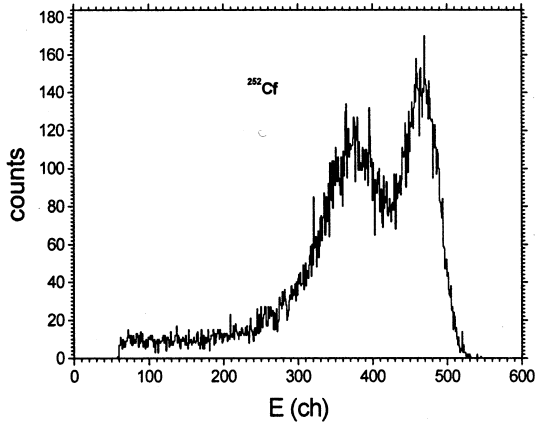

Fig. 14. *Energy spectrum of ^{252}Cf fission fragments*

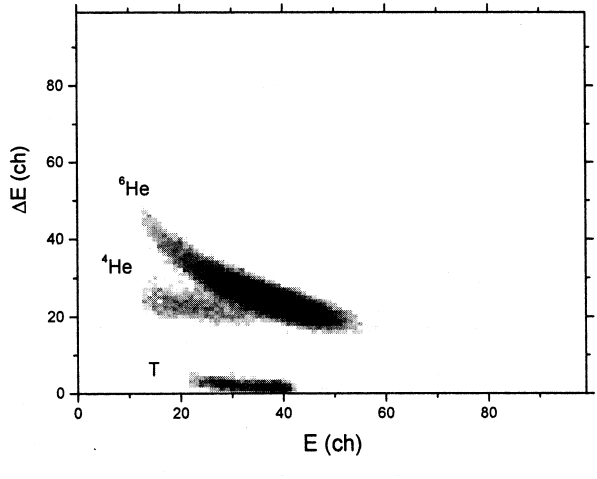

Fig. 15. *(ΔE, E) two-dimensional matrix*

Preliminary results for the elastic scattering and charge exchange reaction of ^{6}He nuclei on the hydrogen-containing target

It is known that elastic scattering measurement allows information on the nucleon distribution in nuclei to be obtained whereas the charge exchange reaction, which links the ground state and the corresponding isobar-analogue state, depends on the degree to which the proton and neutron density distributions differ from each other. By now a few experiments have been carried out on the elastic scattering of ^{6}He on hydrogen [9-11]. Those experiments, in which ^{6}He angular distributions were measured over a narrow angular range, showed that there is a need for elastic scattering to be measured in a wide angular range of Θ_{sm} from 0 to 180° [9]. The wide-aperture set-up outlined in this work is provided with a coordinate system that allows elastic scattering measurement in a wide angular range, including inverse kinematic measurement. Experimental data on the p(^{6}He, ^{6}Li)n charge exchange reaction are simultaneously obtainable as well. In works [12-13], this reaction was studied for ^{6}He ion energies of 560 and 250 MeV, the ^{6}Li angular distributions being also measured in a rather narrow range of forward angles. The set-up under discussion allows measurement in a wider angular range and at essentially lower ^{6}He energies.

To carry out measurement, the configuration shown in Fig. 4 was used. Unified data sets were obtained both for the charge exchange reaction and for elastic scattering, including data on correlated events, inverse geometry being used for scattering measurement.

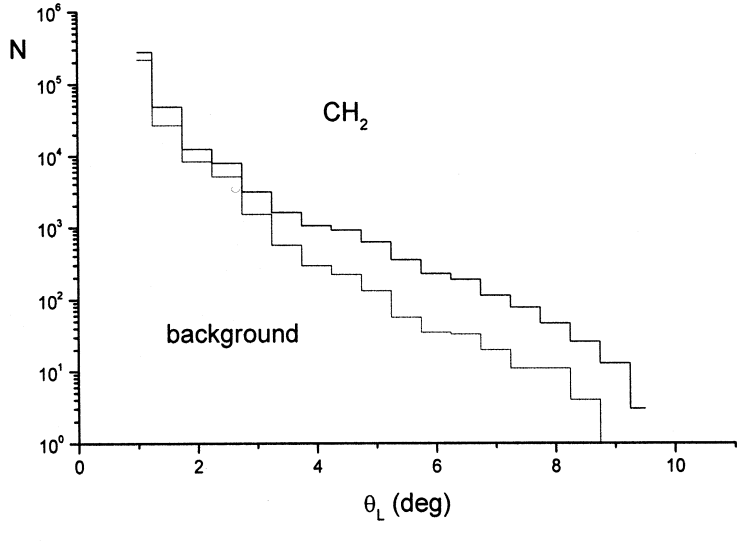

Fig. 16. *Angular distributions of ^{6}He yields*

A secondary 170 MeV beam of ^{6}He was directed at a target positioned as shown in Fig. 4. The beam intensity on the target was ~10^3 1/s, the admixture content of the beam was about (20-30) % tritons. The beam vertical and horizontal dimensions on the target were about 40 and 20 mm (FWHM) respectively, the total angular divergence being less than or equal to $2\theta \approx 2°$ at half-height. Owing to "active" collimation using DC2 (see Fig.6), the dimensions of the incident beam (^{6}He+t) were restricted to about (10x10) mm^2. Trajectory reconstruction and scattering angle measurement for every event were carried out with chambers C1, C3, C5 using standard programs [6].

For reasons of limited time, a relatively thick (x = 1.44 mm) target of CH_2 was used.

Fig. 16 presents the normalised angular distributions (yields) measured with a CH_2 target and without a target (background measurement), which allow background conditions to be taken account for in measurement and data collection. To distinguish ^{6}He, its two-dimensional spectrum (ΔE, E), provided by the set-up spectrometric section, was used.

Presented in Fig. 17 are the (ΔE, E) spectra of CH_2-target-scattered particles. There are three prominent regions of Z = 1, 2, 3 to be interpreted as associated with t, ^{4}He+^{6}He and ^{6}Li. On subtracting the corresponding background data, the ^{6}He scattering and charge exchange cross sections were calculated. They are presented in Fig. 18. The horizontal error is the sum of the scattering angle measurement error and the error due to the angular divergence of the incident beam.

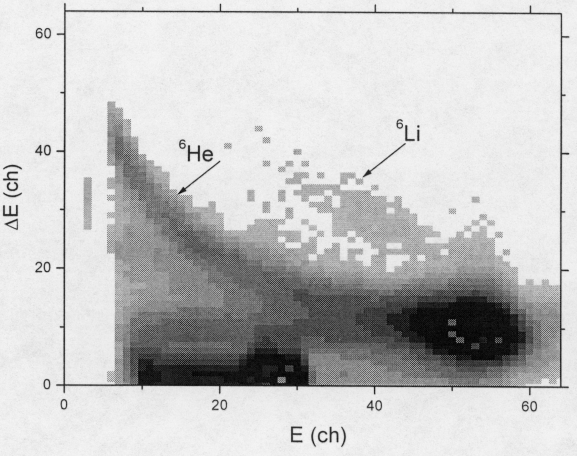

Fig. 17. *Two-dimensional (Δ, E) matrix of CH_2-target-scattered particles*

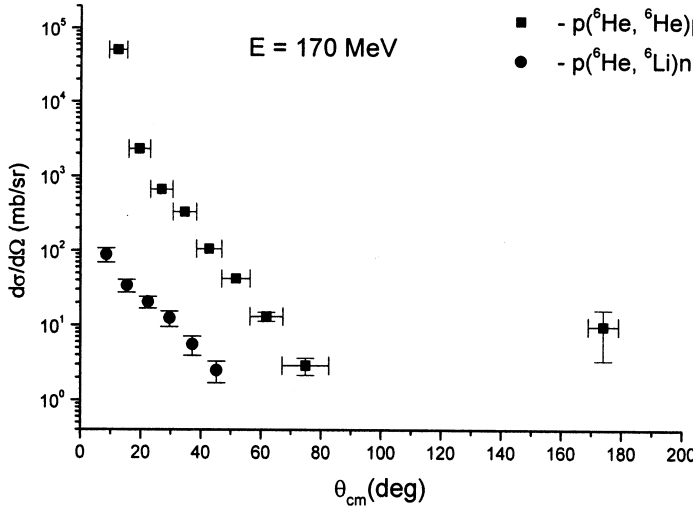

Fig. 18. *Experimental differential cross sections for the elastic scattering and charge exchange of ^6He on the CH_2 target*

The background angular divergence calculated from Fig. 16 is $\sigma(\theta_L) \approx 0.5°$. For the chosen geometry, the accuracy of trajectory reconstruction (angular resolution) is $\sigma(\theta_L) \approx 0.2°$, which is found by simulation using standard programs [6]. The vertical (statistical) errors for the unmarked experimental dots in Fig. 18 can be judged by the dot sizes.

The chosen set-up geometry (target position) restricted angular measurement to $\theta_L<9°$, which corresponds to the limiting value for $\theta_{cm}<78.8°$.

The set-up described, which is based on MWPCs composed of independent detection channels, enables correlated events to be distinguished. This makes it possible to measure the scattering cross sections for ^6He on the proton (from data on CH_2 scattering) by separating correlated (^6He, p) and (^4He, d) pairs in p(^6He, ^6He)p and p(^6He, ^5He)d reactions in inverse kinematics in the angular range $\theta_{cm} \approx (165\text{-}180)°$. The corresponding point in Fig. 18, farthest to the right, is a combined point for both reactions. Considering the indubitable importance of this kind of measurement, the data are presented from which this result was obtained.

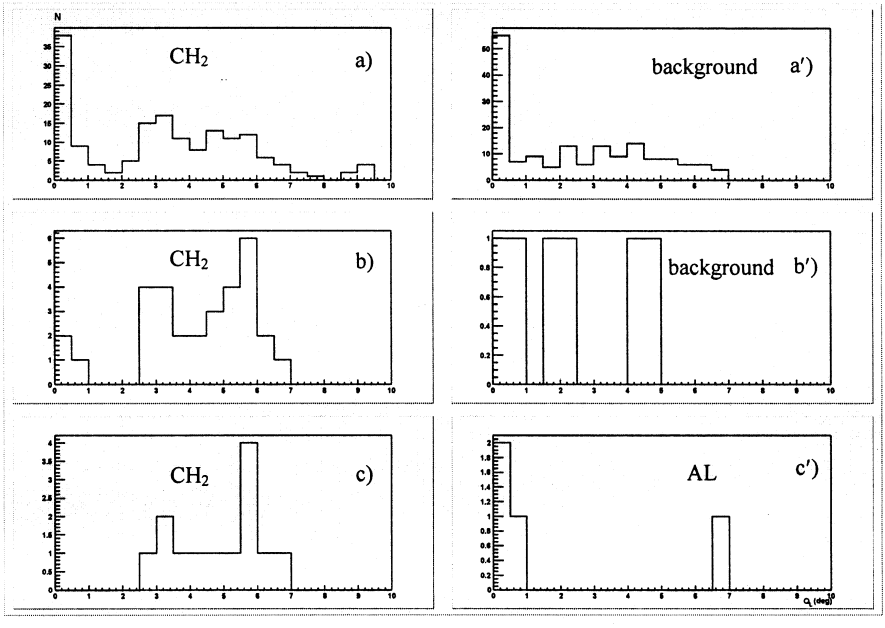

Fig. 19. *Yields of correlated pairs as a function of the angle between them for $p(^6He, ^6He)p$ and $p(^6He, ^5He)d$ reactions. a, b, c - a CH_2 target; a′, b′ - no target; c′ - an aluminium target with an equivalent number of nuclei*

Fig. 19 shows the yields of correlated pairs as a function of the lab frame angle between them:

- Fig. 19a, a′ for the whole (ΔE, E) region on Fig17 associated with Z > 1 . Before calculating the cross section, the background distribution (Fig. 19a′) was subtracted from the distribution on the target, the cross section being averaged over the whole angular range $\Theta_{cm} \approx (165\text{-}180)°$;

- Figs. 19b, b′ for the region in Fig. 17 associated with ^{6}He and ^{4}He scattered in inverse geometry and separated based on their energy release, ΔE. The procedure of separating this region is identical to assigning the ΔE upper threshold for processing. A comparison of Fig. 19b and Fig. 19b′ shows correlated events to be identifiable against primary beam background.

However the most convincing proof is a comparison of the yield of correlated pairs for a hydrogen-free target. Fig. 19c′ shows the yield of pairs for a 2 mm thick aluminium target of an equivalent number of nuclei, and Fig. 19c shows the corresponding normalised yield for CH_2.

To sum up, it is to be noted once again that the whole body of data from Fig. 19a, a′ was used to determine the backward scattering cross sections, whereas Fig. 19b, b′ is convincing proof that the data on backward scattering are reliable.

Conclusions

The MWPC-based set-up was created for measuring the beam profile, reconstructing the trajectories of reaction particles, including the trajectories of correlated particles, in experiments on scattering and the break-up of exotic nuclei into clusters as well for experiments.

The system of MWPCs provides:

- event detection within $\theta_L \approx 30°$ $\varphi \approx 2\pi$, including backward semisphere measurement;
- trigger generation for relatively large scattering angles, $\theta_L \geq 5°$;
- selection of the trajectories associated with a particular scattering centre;
- trigger generation for narrow entrance beam formation ("active collimation);
- initiating particle entrance angle determination;
- beam monitoring for measuring absolute cross sections
- reliable 100% detection of a wide spectrum of nuclei beginning with the proton
- reliable operation for no less than 15 days, the gas parameters remaining unchanged.

The use of a large-aperture LDIC as a ΔE-detector in combination with a CsI E-detector allows to identify and energy measurement for the particles of $Z \geq 1$ and $E \geq 2$ MeV/ A. The fact that correlated reaction particles can be selected against incident beam background and that the angle between correlated pairs can be measured will allow one to obtain unique physics information on scattering within the angle $\theta_{cm} \approx 180°$ in inverse geometry.

The authors express their gratitude to V.V. Shchetinina and V.V Bashevoy for their help in designing the set-up and to the U-400M team for providing the efficient operation of the accelerator. We would like to thank E.G.Biryukov for valuable assistance during the preparation of the present article.

This work was supported by the Russian Fund of Fundamental Research (Grant 01-02-22001) and INTAS (Grant 00-00-463).

References

1.Yu.G.Sobolev, M.P.Ivanov, R.Kalpakchieva et al. Instruments and Experimental Techniques, 1997, V.40, N5, P.589-594.
2.Asaturyan R.A., Astabatyan R.A., Ivanov M.P. et al. Instruments and Experimental Techniques, 1999, V42, N 3, P.342-346.
3. Charpak G. et al, NIM, 62 (1968) , p.262.
4. Lukyanov S.M., Penionzhkevich Yu.E., Kalpakchieva R. et al. Communication of the JINR, P, 13-2000-283, Dubna, 2000. (in Russian)
5. Azhgirei L.S., Zrelov P.V., Ignatenko M.A. et al. Preprint JINR, 13-84-652, Dubna, 1984.
6.Rene Brun and Fons Rademakers, *ROOT - An Object Oriented Data Analysis Framework*, Nucl. Inst. & Meth. in Phys. Res. A 389 (1997) 81-86. See also http://root.cern.ch/.
7. Astabatyan R.A., Badalyan H.V., Demekhina N.A. et al. Proc.Int.Conf. High Energy Exper. and Methods, Bechyne, 1989, p.110.
8. Astabatyan R.A., Gasparyan S.G., Demekchina N.A. et al. Preprint YerPhI-1280(66)-90, Yerevan, 1990. (in Russian)
9. Wolski R., Fomichev A.S., Rodin A.M. et al. Phys.Lett. B467, 8(1999), P.8-14.
10.M.D.Cortina-Gil, P.Roussel-Chomaz, N. Alamanos et al. Phys.Lett. B401, 9(1997).
11. A.deVismes, P.Roussel-Chomaz, et al. Phys.Lett. B505, 15(2001).
12. J.A.Brown, D.Bazin, W.Beneson et al. Phys.Rev. C54, 1999, P.2105.
13. M.D. Cortina-Gil, P.Roussel-Chomaz, N. Alamanos et al. Phys.Lett. B371, 14 (1996).

Received on June 13, 2002.

Астабатян Р. А. и др. E13-2002-138
Установка на основе многопроволочных пропорциональных и ионизационных камер для экспериментов на радиоактивных пучках

Описана широкоапертурная установка, предназначенная для ядерно-физических экспериментов на пучках радиоактивных ядер. Установка включает в себя: многопроволочную пропорциональную камеру (МПК) для измерения профиля пучка, МПК для измерения угловых распределений продуктов реакций, (ΔE,E)-детектор на основе кристалла CsI (Tl) и продольную дрейфовую ионизационную камеру для измерения энергии рассеянных частиц и их идентификации. Приводятся результаты испытаний координатных МПК, а также результаты идентификации частиц на фотонном и ионных пучках и результаты предварительных измерений упругого рассеяния и реакции перезарядки ^{6}He с энергией 170 МэВ на водородосодержащей мишени CH_2.

Работа выполнена в Лаборатории ядерных реакций им. Г. Н. Флерова ОИЯИ.

Препринт Объединенного института ядерных исследований. Дубна, 2002

Astabatyan R. A. et al. E13-2002-138
Set-Up on the Basis of Multiwire Proportional and Ionization Chambers for Radioactive Beam Experiments

A large-aperture set-up designed for nuclear physics experiments on beams of radioactive nuclei is described. The set-up includes Multiwire Proportional Chamber (MWPC) for measuring the beam profile, MWPC for measuring reaction product angular distributions, a CsI (Tl)-crystal detector and a longitudinal drift ionization chamber for identifying scattered particles and measuring their energy. The results of tests of coordinate MWPCs, particle identification on photon and ion beams, and preliminary measurements of the elastic scattering and the charge exchange reaction of 170 MeV ^{6}He on a CH_2 target are presented.

The investigation has been performed at the Flerov Laboratory of Nuclear Reactions, JINR.

Preprint of the Joint Institute for Nuclear Research. Dubna, 2002

Макет *Т. Е. Попеко*

ЛР № 020579 от 23.06.97.
Подписано в печать 27.06.2002.
Формат 60 × 90/16. Бумага офсетная. Печать офсетная.
Усл. печ. л. 1,43. Уч.-изд. л. 2,64. Тираж 335 экз. Заказ № 53378.

Издательский отдел Объединенного института ядерных исследований
141980, г. Дубна, Московская обл., ул. Жолио-Кюри, 6.